Preparation, Characterization, and Antibacterial Activity of Silver Nanoparticle-Decorated Ordered Mesoporous Carbon

Dung Van Nguyen
Faculty of Chemical Engineering, Ho Chi Minh City University of Technology (HCMUT), VNU-HCM, Ho Chi Minh City, Vietnam
nvdung@hcmut.edu.vn (corresponding author)

Duong Thuy Nguyen
Faculty of Chemical Engineering, Ho Chi Minh City University of Technology (HCMUT), VNU-HCM, Ho Chi Minh City, Vietnam
ntduong49@gmail.com

Vi Le Tuong Tran
Faculty of Chemical Engineering, Ho Chi Minh City University of Technology (HCMUT), VNU-HCM, Ho Chi Minh City, Vietnam
vi.tranhoak19@hcmut.edu.vn

Khang Dinh Vo
Faculty of Chemical Engineering, Ho Chi Minh City University of Technology (HCMUT), VNU-HCM, Ho Chi Minh City, Vietnam
khang.vocek19@hcmut.edu.vn

Long Quang Nguyen
Faculty of Chemical Engineering, Ho Chi Minh City University of Technology (HCMUT), VNU-HCM, Ho Chi Minh City, Vietnam
nqlong@hcmut.edu.vn

Received: 14 February 2023 | Revised: 16 March 2023 and 23 April 2023 | Accepted: 24 April 2023

 DOI: https://doi.org/10.48084/etasr.5782

ABSTRACT

In this study, Ordered Mesoporous Carbon (OMC) was prepared using resol as a carbon precursor and F127 as a soft template. Small-angle X-ray Diffraction (XRD), Transmission Electron Microscopy (TEM) images, and nitrogen adsorption and desorption isotherms revealed that OMC possessed ordered hexagonal mesostructures (p6m) with an ordered pore size of 3.2nm, a high specific surface area (S_{BET}) of 539m^2/g, and a large total pore volume (V_{total}) of 0.44cm^3/g. Subsequently, silver nanoparticles synthesized from an aqueous $AgNO_3$ solution using glucose as a reducing agent and starch as a stabilizing agent were decorated on OMC, producing Ag/OMC. XRD analysis revealed that the composite contained silver crystals. In addition, the content and size of silver nanoparticles in Ag/OMC were 0.71wt% (AAS) and around 25-50nm (TEM), respectively. Due to the surface cover of silver nanoparticles, S_{BET} and V_{total} of Ag/OMC slightly decreased to 417m^2/g and 0.38cm^3/g, respectively. Both agar and broth dilution techniques were used to evaluate the antibacterial activity of the material against *Staphylococcus aureus*. Ag/OMC with a Minimum Inhibitory Concentration (MIC) of 25.0µg/mL is a potential candidate for use against *Staphylococcus aureus*.

Keywords-mesoporous carbon; soft template; silver nanoparticles; green synthesis; antibacterial activity; Staphylococcus aureus

I. INTRODUCTION

Over the past few decades, nanomaterials, which exhibit unique nanoscale properties compared to their bulk composition, have propelled research in numerous fields [1-3]. Advances in nanoparticle production in a variety of sizes and shapes have facilitated the expansion of their applications [4-6]. Due to their outstanding physical, chemical, and biological properties, silver nanoparticles have been intensively studied for various uses, such as antibacterial agents, imaging probes, reduction catalysts, and oxidation catalysts [7-9]. To prepare silver nanoparticles, chemical reduction techniques are commonly and extensively used [10], which involve the use of reducing agents like sodium borohydride, hydrazine, and citrate to convert silver ions into silver nanoparticles. These methods provide multiple advantages, including a high yield of silver nanoparticles and the ability to control the size and shape of the nanoparticles. However, the use of toxic chemicals is a significant obstacle. To overcome that problem, different green methods have been explored. Glucose and starch are recognized as natural, renewable, non-toxic, and inexpensive agents [11-12]. Glucose can replace traditional reducing agents, while starch molecules can act as stabilizing agents by adsorbing onto the surface of nanoparticles, preventing their aggregation. As a result, the combination of glucose and starch offers a green and sustainable approach for the preparation of silver nanoparticles with controlled size and shape. However, silver nanoparticles with high surface energy tend to aggregate [13]. As a result, the peculiar properties of these nanoparticles can be drastically diminished during use [14]. To address this issue, silver nanoparticles should be stabilized on appropriate supports to prevent their aggregation [15-16]. In recent years, Ordered Mesoporous Carbon (OMC) with pore diameters ranging from 2 to 50nm has garnered considerable interest due to its higher specific surface area, larger pore volume, electrical and thermal conductivity, chemical inertness, good thermomechanical stability, and various oxygen-containing functional groups [17-18]. Therefore, OMC has been applied in numerous fields, such as adsorption, catalyst support, hydrogen storage, carbon dioxide capture, lithium batteries, electrochemical sensors, electrochemical capacitors, and drug delivery [19-22]. Commonly, OMC can be fabricated by nanocasting using ordered mesoporous silica as a hard template. This method yields OMC with a high specific surface area and a large pore volume [23]. Nevertheless, this process requires the preparation of ordered mesoporous silica in the first step but sacrifices it in a later step [24]. Furthermore, the removal of this template has the potential to damage the surface of the OMC and cause environmental pollution [25]. In general, this method has the drawbacks of being expensive, complicated, and difficult to scale up [26]. A cost-effective and eco-friendly soft-template method was developed to address the limitations of existing technologies. Self-assembly of block copolymers is the basis for OMC production [27]. Carbon precursors (e.g. resol, phenolic resin) are self-assembled into supramolecular aggregates with block copolymers (acting as soft templates, e.g. F127, P123) [28-30]. The mixture is then thermopolymerized to give a cross-linked composite, the template is removed, and carbonization occurs. Resol is a common carbon source for this approach due to its moderate weight and size and its moveability in surfactant environments [23, 31]. F127 has advantages as a versatile and widely used soft template for the preparation of mesoporous materials, including high porosity, tunability, thermal stability, biocompatibility, and ease of use [32-33]. Moreover, F127 can be decomposed easily at low temperatures (e.g. 350°C), while resol is more stable [30]. The template can be removed to leave mesopores. The complete carbonization of resol to obtain the final OMC framework can be conducted at high temperatures (e.g. 600°C).

Several studies have reported the dispersion of silver nanoparticles on mesoporous carbon supports. In [34], silver-decorated mesoporous carbons (CMK-3 type, hard template) were prepared to promote wound healing. In [35], the soft-template method and tetraethyl orthosilicate were used to create mesoporous carbons containing embedded silver nanoparticles. In [36], a silver nanoparticle-OMC composite was prepared using F127 as a soft template and phenolformaldehyde resin as a carbon source, and then applied it to a lithium-ion battery. In [37], a soft template was used to synthesize ordered mesoporous silver nanoparticle/carbon composites for the catalytic reduction of 4-nitrophenol. In general, the use of soft-templated OMC as a support for silver nanoparticles has been rarely reported in the literature. Hence, this research was carried out to investigate the feasibility of incorporating silver nanoparticles and OMC. OMC was first fabricated with F127 as a soft template and resol as the carbon source. The OMC surface was then coated with silver nanoparticles, and the resulting composite was tested for its potential as an antibacterial agent.

II. EXPERIMENTAL PROCEDURE

Phenol (≥99.0%), formaldehyde (37.0-40.0%), $AgNO_3$ (99.8%), and HCl (36.0-38.0%) were purchased from Xilong Scientific Co., Ltd. F127, starch, glucose, and ethanol (≥99.5%) were obtained from BASF, Merk, Guangdong Guanghua Sci-Tech Co. and VN-Chemsol Co., respectively. All chemicals were used as received without any further purification. Resol was produced from phenol and formaldehyde. In a spherical flask, 9.35mL of liquid phenol was magnetically swirled with 1.75mL of a NaOH solution (20wt%). After adding 16.0mL of formaldehyde dropwise, the mixture was agitated continuously for 1 hour at 70°C. After completion of the reaction, the liquid was chilled to room temperature, and the pH was adjusted to approximately 7.0 by adding a 0.6M HCl solution. The water was then vacuumed out at 50°C. The resulting resol was redissolved in ethanol to generate a resol solution (20 wt%), while sodium chloride was separated as a precipitate.

OMC was synthesized from resol as a carbon source and F127 as a soft template. At the beginning, 1.00g of F127 was dissolved in 10.0g of ethanol. Following this, 5.00g of resol solution (20 wt%) were added. After 60 minutes of stirring, the solvent was separated within 24 hours by evaporation at room temperature. The solid was then crushed into a fine powder and placed in a tube furnace with a constant nitrogen flow rate of 70mL/min. Pyrolysis was performed in two consecutive steps: the sample was heated to 350°C at a rate of 2°C/minute and kept at that temperature for 3 hours. Then, it was heated to

600°C at a rate of 5°C/minute and the final temperature was kept for 3 hours. Then, the prepared OMC sample was stored in a plastic bag for further use.

Ag/OMC was prepared by dispersing a colloidal sol of Ag nanoparticles on OMC. At first, a mixture of 1.50mL of $AgNO_3$ (0.100M), 3.00mL of glucose (0.100M), and 90mL of starch solution (0.17 wt%) was heated and stirred at 70°C. After 15 hours of heating and stirring, the sample was collected to determine the formation of Ag nanoparticles using a UV-Vis spectrometer (Spectronic Genesys 2 PC), and then 1.60g of OMC was added to the colloid. The mixture was stirred for 30 minutes and then sonicated. Lastly, the sample was centrifuged, rinsed with distilled water and ethanol, and oven-dried at 60°C for 4 hours. X-ray Diffraction (XRD) measurements were performed on a Bruker AXS D8 diffractometer with Cu-Kα radiation (40kV, 20mA). The morphologies of OMC and Ag/OMC were observed on a JEOL JEM-1400 (100kV) instrument. Nitrogen adsorption and desorption isotherms were conducted on a Quantachrome Autosorb-1 system. Samples were degassed at 300°C for 5 hours. Total pore volume (Vtotal) was calculated at a relative pressure (P/Po) of 0.995. The Brunauer-Emmett-Teller equation was used to determine the specific surface area (S_{BET}). The average pore size ($d_{average}$) was obtained from $4V_{total}/S_{BET}$. The Ag content in Ag/OMC was analyzed with a Shimadzu AA6650 Atomic Absorption Spectrophotometer (AAS).

The antibacterial activity of Ag/OMC was investigated on *Staphylococcus aureus* using two methods: agar dilution and broth dilution. For the agar dilution method, the bacterial strains were grown in Luria-Bertani (LB) medium (peptone 10g/L, yeast extract 5g/L, and NaCl 10g/L) until a density of 10^8CFU/ml was reached (optical density of 0.5 at 600nm). The suspension was then diluted 10 times to obtain a density of 10^7CFU/mL. The bacteria were inoculated on agar plates with different Ag/OMC concentrations. Regarding the broth dilution method, 2mL of LB medium, 100µL of bacteria, and different Ag/OMC concentrations were added into the test tubes. The mixture was shaken at 200rpm and 37°C. For both methods, bacterial growth and Minimum Inhibitory Concentration (MIC) were observed in 24 hours.

III. RESULTS AND DISCUSSION

Small-angle XRD was used to determine the mesoporous structure of OMC, as shown in Figure 1. Several reflections were found in OMC. These reflections at 2θ=0.42, 0.66, and 0.82° correspond to the 10, 11, and 20 planes of the hexagonal (p6m) structure [21-22]. In addition, the high intensities of these peaks suggest that the mesoporous structure is relatively uniform. The TEM images shown in Figure 5(a) reveal that OMC had a well-ordered mesoporous system with trenches running along the plane (110). Compared with [21-22], this morphology of OMC is fairly similar to that of FDU-15 and other 2D hexagonal (p6m) mesoporous materials.

Figure 2 depicts the nitrogen adsorption and desorption isotherms of OMC. As P/P_o increased from 0.01 to 0.71, the adsorbed volume gradually increased, indicating that OMC contained both micropores and mesopores. Next, the adsorbed volume increased very slightly and nearly reached equilibrium at P/P_o, going from 0.71 to 0.99, suggesting that OMC lacked macropores. Notably, a hysteresis loop was long at P/P_o between 0.15-0.71 and wide at P/P_o between 0.36-0.62. This hysteresis loop might belong to type IV, according to the IUPAC classification [38]. Additionally, the shape of the hysteresis loop may be associated with a particular porous structure. This one might be of the H1 type, which represents uniform, open-ended cylinder pores in a 2-D hexagonal structure [39-41]. The BJH pore size distribution shows that OMC had relatively uniform mesopores at 3.2nm and certain micropores, possibly in the mesopore walls. Table I also shows that OMC possessed a high S_{BET}=539m^2/g and a large V_{total}=0.44cm^3/g.

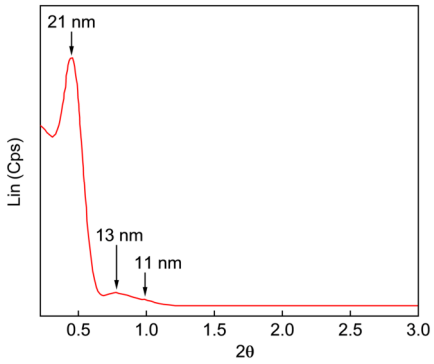

Fig. 1. Small angle X-ray diffraction of OMC.

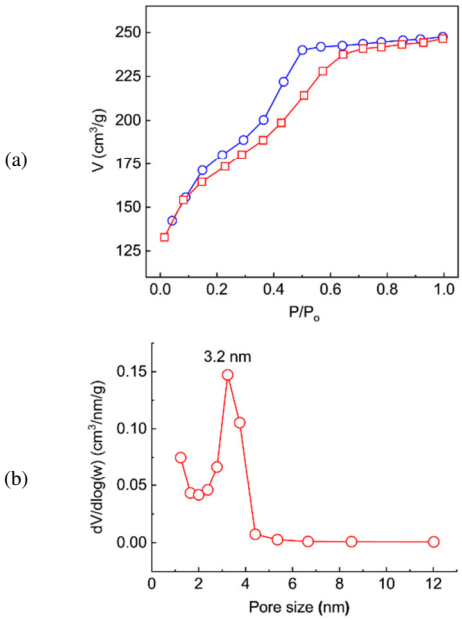

Fig. 2. (a) Nitrogen adsorption and desorption isotherms and (b) BJH pore size distribution of OMC.

TABLE I. PROPERTIES OF OMC AND AG/OMC

Sample	S_{BET} (m^2/g)	V_{total} (cm^3/g)	d_{pore} (nm)	$d_{average}$ (nm)	Ag (wt%)
OMC	539	0.44	3.2	3.3	-
Ag/OMC	417	0.38	-	3.6	0.71

The surface plasmon resonance of the silver nanoparticles allowed the exploration of their formation using UV-Vis absorption in the 350-625nm range, as shown in Figure 3. Colloidal silver had a broad absorption band centered at approximately 418nm and a light yellow color. These observations demonstrated the successful generation of silver nanoparticles. Moreover, the broadband signal revealed a high polydispersity of silver nanoparticles in size and shape. The detailed morphology of the silver nanoparticles was observed together with OMC in the Ag/OMC sample.

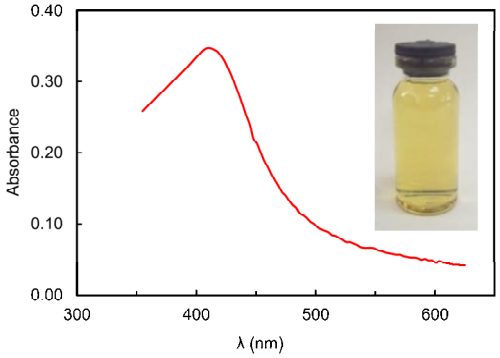

Fig. 3. UV-Vis spectroscopy of silver nanoparticle suspension and its yellow color.

Figure 4 shows the XRD pattern of Ag/OMC to determine its crystal phases. Face-centered cubic silver planes (111), (200), and (220) were represented by distinct peaks at 2θ= 38.3, 44.5, and 64.2°, respectively (JCPDS Card No. 04-0783). Consequently, only silver nanocrystals were found on OMC. Theoretically, based on the amounts of $AgNO_3$ and OMC used, the maximum amount of Ag in Ag/OMC was calculated to be 1.01wt%. The AAS results, however, indicate that the silver content was only 0.71wt%. As a result, approximately 70% of the silver was coated on the surface of the OMC, and the remainder was possibly removed during cleaning.

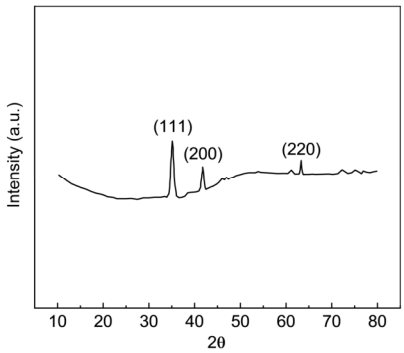

Fig. 4. X-ray diffraction of Ag/OMC.

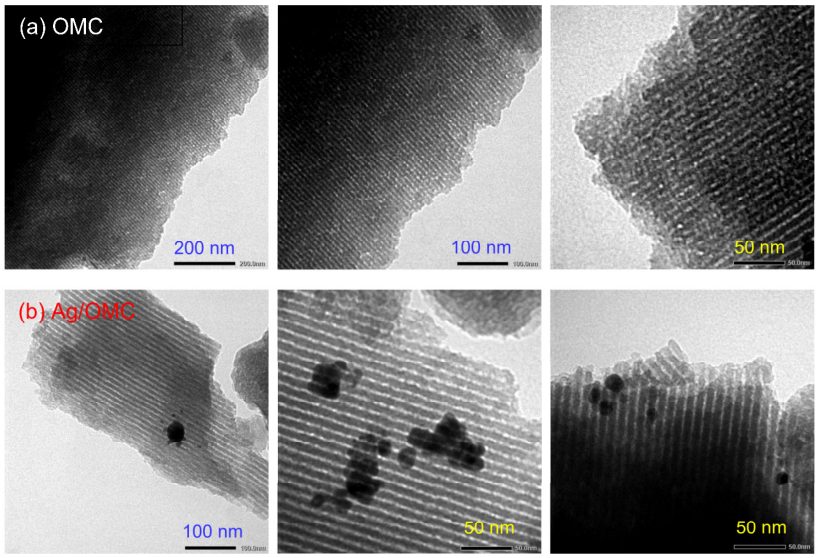

Fig. 5. TEM images of (a) OMC and (b) Ag/OMG

Figure 5 shows TEM images of OMC and Ag/OMC samples. Compared to OMC, the presence of dark spots in the Ag/OMC showed the morphology of silver nanoparticles. In general, a wide size range of 20-50nm was observed for silver nanoparticles of various shapes. As only 0.71wt% of the silver nanoparticles were loaded on the OMC surface, their density was relatively low. Therefore, the stripe-like structure of the OMC was still exposed. In addition, S_{BET} and V_{total} of Ag/OMC were 417m^2/g and 0.38cm^3/g, respectively, which were slightly lower than those of OMC. These decreases were not significant, since silver nanoparticles could have low surface coverage. Thus, the porosity of OMC could be advantageous.

Staphylococcus aureus was used to assess the antibacterial activity of Ag/OMC using both agar and broth dilution methods. Figure 6 and Table II show that the bacteria were not found on agar plates at Ag/OMC concentrations of 25.0 and 50.0μg/mL. Certain bacteria growths were observed at low Ag/OMC concentrations of 0.10-12.5μg/mL. Therefore, the MIC for Ag/OMC was 25.0μg/mL. Figure 7 and Table III

show the results of the broth method. After 24 hours of shaking, the bacteria still caused turbidity in tubes 4-10, showing that they survived at low Ag/OMC concentrations of 0.20-12.5μg/mL. The antibacterial ability of Ag/OMC became effective at higher concentrations of 25.0, 50.0, and 100μg/mL. The mixtures in tubes 1, 2, and 3 were transparent, showing that *Staphylococcus aureus* could not grow. Hence, both methods resulted in similar MICs of 25.0μg/mL. The antibacterial ability of Ag/OMC (0.71wt% Ag) against *Staphylococcus aureus* was generally comparable to those of Ag/activated carbon (0.92wt% Ag, 10μg/mL) [42], Ag/carbon dots (5.4wt% C and 94.6wt% Ag, 20μg/mL) [43], and better than silver nanoparticles prepared by different routes (a broad range of 0.25-430μg/mL) [44]. The dispersion of silver nanoparticles on OMC could prevent their ability to agglomerate, possibly resulting in their enhanced antibacterial activity.

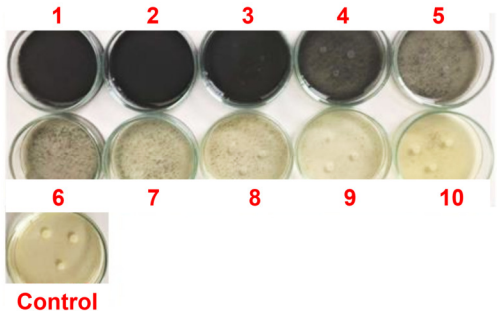

Fig. 6. Experimental image of the agar dilution method.

TABLE II. RESULTS OF AGAR DILUTION METHOD

Control	Concentration (μg/mL)									
	50.0	**25.0**	**12.5**	**6.25**	**3.13**	**1.56**	**0.78**	**0.39**	**0.20**	**0.10**
C	1	2	3	4	5	6	7	8	9	10
+	-	-	+	+	+	+	+	+	+	+

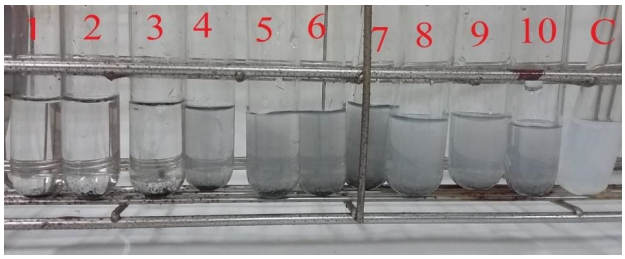

Fig. 7. Experimental image of the broth dilution method.

TABLE III. RESULTS OF BROTH DILUTION METHOD

Control	Concentration (μg/mL)									
	100	**50.0**	**25.0**	**12.5**	**6.25**	**3.13**	**1.56**	**0.78**	**0.39**	**0.20**
C	1	2	3	4	5	6	7	8	9	10
+	-	-	-	+	+	+	+	+	+	+

IV. CONCLUSION

This study successfully fabricated silver nanoparticle-coated ordered mesoporous carbon. At first, resol was used to synthesize OMC using F127 as a soft template. OMC was composed of a mesoporous p6m structure with a typical pore size of 3.2nm, S_{BET}=539m^2/g, and V_{total}=0.44cm^3/g. The surface of OMC was then decorated with silver nanoparticles prepared from $AgNO_3$ using glucose as a reducing agent and starch as a stabilizing agent. TEM images showed that silver nanoparticles with rough sizes of 20-50nm adhered to the surface of OMC. Finally, as shown with a MIC of 25.0μg/mL against *Staphylococcus aureus*, Ag/OMC is expected to have the potential for antibacterial applications.

ACKNOWLEDGEMENT

This research is funded by Vietnam National University HoChiMinh City (VNU-HCM) under grant number: 562-2023-20-04. We acknowledge Ho Chi Minh City University of Technology (HCMUT), VNU-HCM for supporting this study.

REFERENCES

[1] N. Baig, I. Kammakakam, and W. Falath, "Nanomaterials: a review of synthesis methods, properties, recent progress, and challenges," *Materials Advances*, vol. 2, no. 6, pp. 1821–1871, 2021, https://doi.org/10.1039/D0MA00807A.

[2] M. Alavi and M. Rai, "Recent progress in nanoformulations of silver nanoparticles with cellulose, chitosan, and alginic acid biopolymers for antibacterial applications," *Applied Microbiology and Biotechnology*, vol. 103, no. 21, pp. 8669–8676, Nov. 2019, https://doi.org/10.1007/s00253-019-10126-4.

[3] S. M. Alsaedy and N. Aljalawi, "The Effect of Nanomaterials on the Properties of Limestone Dust Green Concrete," *Engineering, Technology & Applied Science Research*, vol. 11, no. 5, pp. 7619–7623, Oct. 2021, https://doi.org/10.48084/etasr.4371.

[4] S. Dawadi *et al.*, "Current Research on Silver Nanoparticles: Synthesis, Characterization, and Applications," *Journal of Nanomaterials*, vol. 2021, Feb. 2021, Art. no. e6687290, https://doi.org/10.1155/2021/6687290.

[5] H. B. Lanjwani, M. S. Chandio, K. Malik, and M. M. Shaikh, "Stability Analysis of Boundary Layer Flow and Heat Transfer of Fe2O3 and Fe-Water Base Nanofluid over a Stretching/Shrinking Sheet with Radiation Effect," *Engineering, Technology & Applied Science Research*, vol. 12, no. 1, pp. 8114–8122, Feb. 2022, https://doi.org/10.48084/etasr.4649.

[6] N. Zaman, S. Ahmed, M. Sanaullah, A. U. Rehman, A. R. Shar, and M. R. Luhur, "Fabrication and Characterization of Organoclay Reinforced Polyester Based Hybrid Nanocomposite Materials," *Engineering, Technology & Applied Science Research*, vol. 8, no. 3, pp. 3038–3040, Jun. 2018, https://doi.org/10.48084/etasr.1977.

[7] S. Kaabipour and S. Hemmati, "A review on the green and sustainable synthesis of silver nanoparticles and one-dimensional silver nanostructures," *Beilstein Journal of Nanotechnology*, vol. 12, no. 1, pp. 102–136, Jan. 2021, https://doi.org/10.3762/bjnano.12.9.

[8] S. Akhtar, Z. Farid, H. Ahmed, S. A. Khan, and Z. N. Khan, "Low-Cost Synthesis and Characterization of Silver Nanoparticles for Diverse Sensing Application," *Engineering, Technology & Applied Science Research*, vol. 9, no. 2, pp. 3915–3917, Apr. 2019, https://doi.org/10.48084/etasr.2450.

[9] V. R. K. R. Galarpe and G. D. Leopoldo, "Potential Recovery of Silver (Ag) from X-ray Fixer Waste by Alkaline Treatment," *Engineering, Technology & Applied Science Research*, vol. 7, no. 5, pp. 2094–2097, Oct. 2017, https://doi.org/10.48084/etasr.1526.

[10] H. D. Beyene, A. A. Werkneh, H. K. Bezabh, and T. G. Ambaye, "Synthesis paradigm and applications of silver nanoparticles (AgNPs), a review," *Sustainable Materials and Technologies*, vol. 13, pp. 18–23, Sep. 2017, https://doi.org/10.1016/j.susmat.2017.08.001.

[11] P. Raveendran, J. Fu, and S. L. Wallen, "A simple and 'green' method for the synthesis of Au, Ag, and Au–Ag alloy nanoparticles," *Green Chemistry*, vol. 8, no. 1, pp. 34–38, 2006, https://doi.org/10.1039/B512540E.

[12] P. Raveendran, J. Fu, and S. L. Wallen, "Completely 'Green' Synthesis and Stabilization of Metal Nanoparticles," *Journal of the American Chemical Society*, vol. 125, no. 46, pp. 13940–13941, Nov. 2003, https://doi.org/10.1021/ja029267j.

[13] C. V. Restrepo and C. C. Villa, "Synthesis of silver nanoparticles, influence of capping agents, and dependence on size and shape: A review," *Environmental Nanotechnology, Monitoring & Management*, vol. 15, May 2021, Art. no. 100428, https://doi.org/10.1016/j.enmm.2021.100428.

[14] A. N. T. Le *et al.*, "Facile Preparation of Multifunctional Ag-Fe_xO_y/C Composite from Coffee Husk for Antibacterial and Catalytic Applications," *Advances in Science and Technology*, vol. 122, pp. 3–9, 2023, https://doi.org/10.4028/p-58b9m3.

[15] G. Liao, J. Fang, Q. Li, S. Li, Z. Xu, and B. Fang, "Ag-Based nanocomposites: synthesis and applications in catalysis," *Nanoscale*, vol. 11, no. 15, pp. 7062–7096, Apr. 2019, https://doi.org/10.1039/C9NR01408J.

[16] N. T. Luon, L. N. Q. Tu, and N. Q. Long, "Catalytic oxidation of formaldehyde over silver supported on ZSM-5: The role of Ag and mesopores," *IOP Conference Series: Earth and Environmental Science*, vol. 964, no. 1, Jan. 2022, Art. no. 012026, https://doi.org/10.1088/1755-1315/964/1/012026.

[17] Z. J. Liang, Z. B. Hong, M. Y. Xie, and D. Gu, "Recent progress on mesoporous carbon materials used in electrochemical catalysis," *New Carbon Materials*, vol. 37, no. 1, pp. 152–179, Feb. 2022, https://doi.org/10.1016/S1872-5805(22)60575-4.

[18] A. Walcarius, "Recent Trends on Electrochemical Sensors Based on Ordered Mesoporous Carbon," *Sensors*, vol. 17, no. 8, Aug. 2017, Art. no. 1863, https://doi.org/10.3390/s17081863.

[19] J. Zhang *et al.*, "Modification of ordered mesoporous carbon for removal of environmental contaminants from aqueous phase: A review," *Journal of Hazardous Materials*, vol. 418, Sep. 2021, Art. no. 126266, https://doi.org/10.1016/j.jhazmat.2021.126266.

[20] D. Gang, Z. Uddin Ahmad, Q. Lian, L. Yao, and M. E. Zappi, "A review of adsorptive remediation of environmental pollutants from aqueous phase by ordered mesoporous carbon," *Chemical Engineering Journal*, vol. 403, Jan. 2021, Art. no. 126286, https://doi.org/10.1016/j.cej.2020.126286.

[21] S. Mehdipour-Ataei and E. Aram, "Mesoporous Carbon-Based Materials: A Review of Synthesis, Modification, and Applications," *Catalysts*, vol. 13, no. 1, Jan. 2023, Art. no. 2, https://doi.org/10.3390/catal13010002.

[22] D. V. Nguyen and H. N. Nguyen "Activation of Mesoporous Carbon Synthesized from SBA-16 for CO_2 Storage," *Vietnam Journal of Chemistry*, vol. 51, no. 4AB, pp. 129-134, Aug. 2013.

[23] C. Liang, Z. Li, and S. Dai, "Mesoporous Carbon Materials: Synthesis and Modification," *Angewandte Chemie International Edition*, vol. 47, no. 20, pp. 3696–3717, 2008, https://doi.org/10.1002/anie.200702046.

[24] G. Collins, P. R. Kasturi, R. Karthik, J.-J. Shim, R. Sukanya, and C. B. Breslin, "Mesoporous carbon-based materials and their applications as non-precious metal electrocatalysts in the oxygen reduction reaction," *Electrochimica Acta*, vol. 439, Jan. 2023, Art. no. 141678, https://doi.org/10.1016/j.electacta.2022.141678.

[25] T.-Y. Ma, L. Liu, and Z. Y. Yuan, "Direct synthesis of ordered mesoporous carbons," *Chemical Society Reviews*, vol. 42, no. 9, pp. 3977–4003, Apr. 2013, https://doi.org/10.1039/C2CS35301F.

[26] M. R. Benzigar *et al.*, "Recent advances in functionalized micro and mesoporous carbon materials: synthesis and applications," *Chemical Society Reviews*, vol. 47, no. 8, pp. 2680–2721, Apr. 2018, https://doi.org/10.1039/C7CS00787F.

[27] A. Saleem, Y. Zhang, M. Usman, M. Haris, and P. Li, "Tailored architectures of mesoporous carbon nanostructures: From synthesis to applications," *Nano Today*, vol. 46, Oct. 2022, Art. no. 101607, https://doi.org/10.1016/j.nantod.2022.101607.

[28] P. Zhang, J. Zhang, and S. Dai, "Mesoporous Carbon Materials with Functional Compositions," *Chemistry – A European Journal*, vol. 23, no. 9, pp. 1986–1998, 2017, https://doi.org/10.1002/chem.201602199.

[29] M. Li and J. Xue, "Ordered mesoporous carbon nanoparticles with well-controlled morphologies from sphere to rod via a soft-template route," *Journal of Colloid and Interface Science*, vol. 377, no. 1, pp. 169–175, Jul. 2012, https://doi.org/10.1016/j.jcis.2012.03.085.

[30] D. V. Nguyen, D. L. T. Nguyen, and H. N. Nguyen, "Soft-Template Synthesis of Mesoporous Carbon and its Gold Supported Derivative as Catalyst for Oxidation of Styrene to Benzaldehyde," *Vietnam Journal of Chemistry*, vol. 51, no. 4AB, pp. 123–128, Aug. 2013.

[31] K. S. Lakhi *et al.*, "Mesoporous carbon nitrides: synthesis, functionalization, and applications," *Chemical Society Reviews*, vol. 46, no. 1, pp. 72–101, 2017, https://doi.org/10.1039/C6CS00532B.

[32] S. Lu *et al.*, "Soft template synthesis of honeycomb-like ratiometric oxygen sensitive polystyrene nanospheres and their application in anti-counterfeit authentication and food packaging dynamic indication," *Sensors and Actuators B: Chemical*, vol. 232, pp. 585–594, Sep. 2016, https://doi.org/10.1016/j.snb.2016.04.007.

[33] Z. Qiu, N. Huang, X. Ge, J. Xuan, and P. Wang, "Preparation of N-doped nano-hollow capsule carbon nanocage as ORR catalyst in alkaline solution by PVP modified F127," *International Journal of Hydrogen Energy*, vol. 45, no. 15, pp. 8667–8675, Mar. 2020, https://doi.org/10.1016/j.ijhydene.2020.01.112.

[34] E. Torre *et al.*, "Silver Decorated Mesoporous Carbons for the Treatment of Acute and Chronic Wounds, in a Tissue Regeneration Context," *International Journal of Nanomedicine*, vol. 14, pp. 10147–10164, Dec. 2019, https://doi.org/10.2147/IJN.S234393.

[35] J. Choma, K. Jedynak, J. Górka, and M. Jaroniec, "Soft-templating synthesis and adsorption properties of mesoporous carbons with embedded silver nanoparticles," *Adsorption*, vol. 17, no. 3, pp. 461–466, Jun. 2011, https://doi.org/10.1007/s10450-010-9292-4.

[36] Y. C. Tsai and R. Doong, "Hierarchically ordered mesoporous carbons and silver nanoparticles as asymmetric electrodes for highly efficient capacitive deionization," *Desalination*, vol. 398, pp. 171–179, Nov. 2016, https://doi.org/10.1016/j.desal.2016.07.029.

[37] Y. Chi, J. Tu, M. Wang, X. Li, and Z. Zhao, "One-pot synthesis of ordered mesoporous silver nanoparticle/carbon composites for catalytic reduction of 4-nitrophenol," *Journal of Colloid and Interface Science*, vol. 423, pp. 54–59, Jun. 2014, https://doi.org/10.1016/j.jcis.2014.02.029.

[38] K. S. W. Sing, "Reporting physisorption data for gas/solid systems with special reference to the determination of surface area and porosity (Recommendations 1984)," *Pure and Applied Chemistry*, vol. 57, no. 4, pp. 603–619, Jan. 1985, https://doi.org/10.1351/pac198557040603.

[39] Y. Meng *et al.*, "A Family of Highly Ordered Mesoporous Polymer Resin and Carbon Structures from Organic–Organic Self-Assembly," *Chemistry of Materials*, vol. 18, no. 18, pp. 4447–4464, Sep. 2006, https://doi.org/10.1021/cm060921u.

[40] T. Horikawa, D. D. Do, and D. Nicholson, "Capillary condensation of adsorbates in porous materials," *Advances in Colloid and Interface Science*, vol. 169, no. 1, pp. 40–58, Nov. 2011, https://doi.org/10.1016/j.cis.2011.08.003.

[41] V.-D. Nguyen, T.-T.-T. Nguyen, T.-M. Tran-Thuy, H.-H. Lam, and Q.-L. Nguyen, "Activation of ordered mesoporous carbon nitride prepared via soft-template for CO_2 adsorption," in *IOP Conference Series: Earth and Environmental Science*, Ho Chi Minh City, Vietnam, Sep. 2021, vol. 947, Art. no. 012034, https://doi.org/10.1088/1755-1315/947/1/012034.

[42] W. Wang, K. Xiao, T. He, and L. Zhu, "Synthesis and characterization of Ag nanoparticles decorated mesoporous sintered activated carbon with antibacterial and adsorptive properties," *Journal of Alloys and Compounds*, vol. 647, pp. 1007–1012, Oct. 2015, https://doi.org/10.1016/j.jallcom.2015.05.180.

[43] P. Wang, Y. Song, Q. Mei, W.-F. Dong, and L. Li, "Sliver nanoparticles@carbon dots for synergistic antibacterial activity," *Applied Surface Science*, vol. 600, Oct. 2022, Art. no. 154125, https://doi.org/10.1016/j.apsusc.2022.154125.

[44] E. O. Mikhailova, "Silver Nanoparticles: Mechanism of Action and Probable Bio-Application," *Journal of Functional Biomaterials*, vol. 11, no. 4, Dec. 2020, Art. no. 84, https://doi.org/10.3390/jfb11040084.